pNRQCD EFT and application to phenomenology

Quarkonia as Tools

Peter Vander Griend

based on JHEP 05 (2021) 136 and Phys. Rev. D 104 (2021) 9, 094049

in collaboration with Nora Brambilla, Miguel Escobedo, Michael Strickland, Antonio Vairo, and Johannes Weber

Technical University of Munich

14 January 2022

Introduction

Motivation: use heavy quarks and their bound states to probe the strongly coupled medium formed in heavy ion collisions

- high mass M of bottom quarks and the short formation time of their bound states make them ideal probes of the quark gluon plasma (QGP); observables of interest include nuclear suppression factor R_{AA} and elliptic flow v_2
- ideally suited for treatment using the formalism of open quantum systems (OQS) and effective field theory (EFT)
  - OQS: allows for the rigorous treatment of a quantum system of interest (heavy quarkonium) coupled to an environment (QGP)
  - EFTs: take advantage of the large mass of the heavy quark and the resulting nonrelativistic nature of the system and small bound state radius using potential nonrelativistic QCD (pNRQCD), an EFT of the strong interaction

Advantages: fully quantum, non-Abelian, heavy quark number conserving, account for dissociation and recombination, and valid for strong or weak coupling

Physical Setup

relevant energy scales (EFT)

- heavy quark mass $M = M_b \sim 5$ GeV
- inverse Bohr radius $1/a_0 \sim 1.5$ GeV
- (π times) the temperature of the medium $(\pi)T \sim 1.5$ GeV
- (Coulombic) binding energy $E \sim 0.5$ GeV
- hierarchical ordering: $M \gg 1/a_0 \gg (\pi)T \gg E$ [1]

relevant time scales (OQS)

- system intrinsic time scale: $\tau_S \sim 1/E$
- environment correlation time: $\tau_E \sim 1/(\pi T)$
- relaxation time: $\tau_R \sim 1/\Sigma_s \sim 1/(a_0^2(\pi T)^3)$ (where Σ_s is the thermal self energy)

[1] $\pi T \sim 1.5$ GeV at initial time; medium quickly expands and cools such that $1/a_0 \gg \pi T$ is realized

Hierarchies and Simplifying Assumptions

quantum Brownian motion

for

$$\tau_R, \tau_S \gg \tau_E,$$

where τ_R, τ_S, and τ_E are the relaxation, system intrinsic, and environment correlation time scales, respectively, the system realizes **quantum Brownian motion**

Simplifying Approximations

hierarchy of scales allows for two simplifying approximations:

- **Born approximation**: quarkonium has little effect on the medium at time scales of interest; density matrix factorizes, i.e., $\rho(t) \propto \rho_S(t) \otimes \rho_E$
- **Markov approximation**: only the state of the quarkonium at the present time is necessary to describe its evolution, i.e., no memory integral

potential Non-Relativistic QCD (pNRQCD)

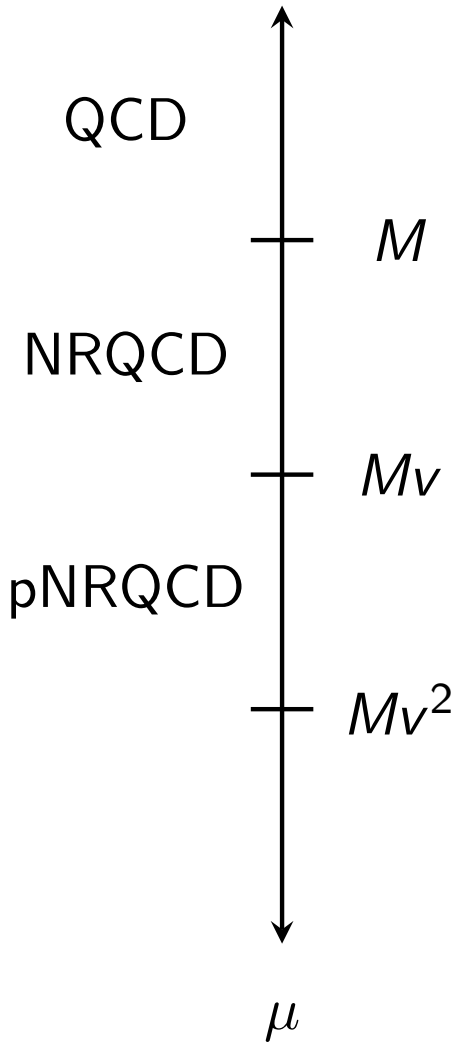

- effective theory of the strong interaction obtained from full QCD via non-relativistic QCD (NRQCD) by successive integrating out of the hard (M) and soft (Mv) scales where $v \ll 1$ is the relative velocity in a heavy-heavy bound state
- degrees of freedom are singlet and octet heavy-heavy bound states and ultrasoft gluons
- small bound state radius and large quark mass allow for double expansion in r and M^{-1} at the Lagrangian level

pNRQCD Lagrangian[2]

$$\mathcal{L}_{\text{pNRQCD}} = \text{Tr}\Big[S^\dagger (i\partial_0 - h_s) S + O^\dagger (iD_0 - h_o) O + O^\dagger \mathrm{r}\cdot g\,\mathrm{E}\, S + S^\dagger \mathrm{r}\cdot g\,\mathrm{E}\, O + \frac{1}{2} O^\dagger \left\{ \mathbf{r}\cdot g\,\mathrm{E}\,,\, O \right\} \Big]$$

- singlet and octet field S and O interacting via chromo-electric dipole vertices
- $h_{s,o} = \frac{\mathrm{p}^2}{M} + V_{s,o}$: singlet, octet Hamiltonian
  - $V_s = -\frac{C_f \alpha_s(1/a0)}{r}$: attractive singlet potential
  - $V_o = \frac{\alpha_s(1/a0)}{2N_c r}$: repulsive octet potential
- $iD_0 O = i\partial_0 O - [gA_0, O]$
  - commutator can be eliminated via field redefinition

$$E^{a,i}(s,\mathbf{0}) \to \tilde{E}^{a,i}(s,\mathbf{0}) = \Omega(s) E^{a,i}(s,\mathbf{0}) \Omega(s)^\dagger$$

where

$$\Omega(s) = \exp\left[-ig \int_{-\infty}^{s} \mathrm{d}s' A_0(s',\mathbf{0}) \right]$$

[2] Brambilla, Pineda, Soto, Vairo: Nucl.Phys.B 566 (2000) 275; Rev.Mod.Phys. 77 (2005) 1423

Evolution Equations[3]

evolution equations of in-medium Coulombic heavy quarkonium given by:

$$\frac{\mathrm{d}\rho_s(t)}{\mathrm{d}t} = -i\,[h_s, \rho_s(t)] - \Sigma_s\rho_s(t) - \rho_s(t)\Sigma_s^\dagger + \Xi_{so}(\rho_o(t))$$

$$\frac{\mathrm{d}\rho_o(t)}{\mathrm{d}t} = -i\,[h_o, \rho_o(t)] - \Sigma_o\rho_o(t) - \rho_o(t)\Sigma_o^\dagger + \Xi_{os}(\rho_s(t)) + \Xi_{oo}(\rho_o(t))$$

where the Σ and Ξ encode interactions with the medium and can be computed diagrammatically in pNRQCD

[3] Brambilla, Escobedo, Soto, Vairo: Phys. Rev. D 97 (2018) 7, 074009

Diagrammatic Evolution of $\rho_s(t)$

singlet evolution given by

$$\frac{\mathrm{d}\rho_s(t)}{\mathrm{d}t} = -i\left[h_s, \rho_s(t)\right] - \Sigma_s\rho_s(t) - \rho_s(t)\Sigma_s^\dagger + \Xi_{so}(\rho_o(t))$$

where

$\Sigma_s\rho_s(t) \sim$

$\Xi_{so}(\rho_o(t)) \sim$

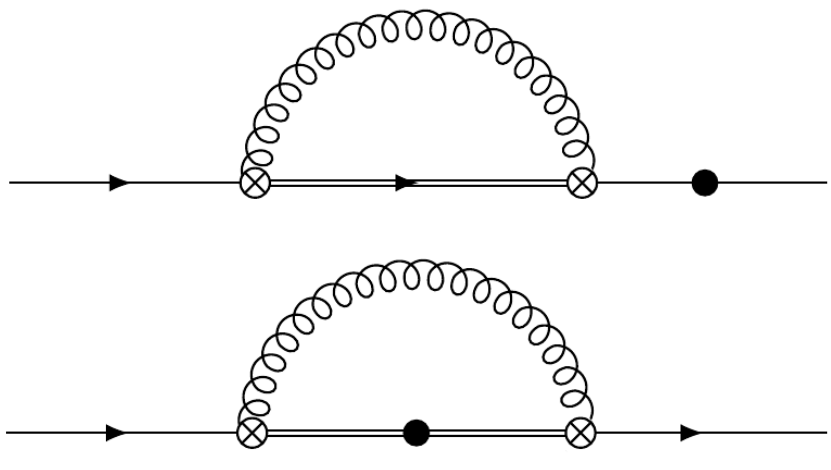

Diagramatic Evolution of $\rho_o(t)$

octet evolution given by

$$\frac{\mathrm{d}\rho_o(t)}{\mathrm{d}t} = -i\left[h_o, \rho_o(t)\right] - \Sigma_o\rho_o(t) - \rho_o(t)\Sigma_o^\dagger + \Xi_{os}(\rho_s(t)) + \Xi_{oo}(\rho_o(t))$$

where

$\Sigma_o\rho_o(t) \sim$

$\Xi_{os}(\rho_s(t)) \sim$

$\Xi_{oo}(\rho_o(t)) \sim$

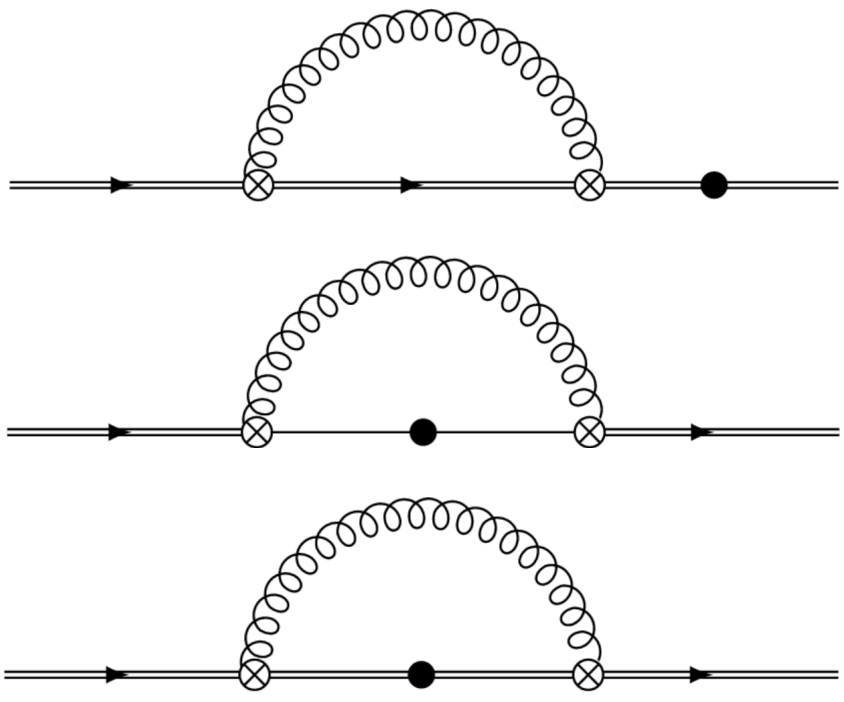

Master Equation

evolution equations can be rewritten as master equation

$$\frac{\mathrm{d}\rho(t)}{\mathrm{d}t} = -i[H,\rho(t)] + \sum_{n,m} h_{nm}\left(L_i^n \rho(t) L_i^{m\dagger} - \frac{1}{2}\left\{L_i^{m\dagger}L_i^n, \rho(t)\right\}\right),$$

where

$$\rho(t) = \begin{pmatrix} \rho_s(t) & 0 \\ 0 & \rho_o(t) \end{pmatrix}, \quad H = \begin{pmatrix} h_s + \mathrm{Im}(\Sigma_s) & 0 \\ 0 & h_o + \mathrm{Im}(\Sigma_o) \end{pmatrix},$$

$$L_i^0 = \begin{pmatrix} 0 & 0 \\ 0 & 1 \end{pmatrix} r^i, \quad L_i^1 = \begin{pmatrix} 0 & 0 \\ 0 & \frac{N_c^2-4}{2(N_c^2-1)} A_i^{oo\dagger} \end{pmatrix}, \quad L_i^2 = \begin{pmatrix} 0 & \frac{1}{\sqrt{N_c^2-1}} \\ 1 & 0 \end{pmatrix} r^i,$$

$$L_i^3 = \begin{pmatrix} 0 & \frac{1}{\sqrt{N_c^2-1}} A_i^{os\dagger} \\ A_i^{so\dagger} & 0 \end{pmatrix}, \quad h = \begin{pmatrix} 0 & 1 & 0 & 0 \\ 1 & 0 & 0 & 0 \\ 0 & 0 & 0 & 1 \\ 0 & 0 & 1 & 0 \end{pmatrix},$$

$$\boxed{A_i^{uv} = \frac{g^2}{6N_c}\int_0^\infty \mathrm{d}s\, e^{-ih_u s} r^i e^{ih_v s} \langle \tilde{E}^{a,j}(0,\mathbf{0}) \tilde{E}^{a,j}(s,\mathbf{0})\rangle}$$

Lindblad Equation

- for $(\pi)T \gg E$, $e^{-ih_{s,o}s} \approx 1$ and medium interactions simplify

$$A_i^{uv} = \frac{r^i}{2}(\kappa - i\gamma),$$

where

$$\kappa = \frac{g^2}{6N_c}\int_0^\infty \mathrm{d}t \left\langle \left\{ \tilde{E}^{a,i}(t,0), \tilde{E}^{a,i}(0,0) \right\} \right\rangle,$$
$$\gamma = -\frac{ig^2}{6N_c}\int_0^\infty \mathrm{d}t \left\langle \left[\tilde{E}^{a,i}(t,0), \tilde{E}^{a,i}(0,0) \right] \right\rangle$$

- as shown by Casalderrey-Solana and Teaney, κ is the heavy quark momentum diffusion coefficient occurring in a Langevin equation describing the diffusion of a single heavy quark[4]; γ is its dispersive counterpart
- master equation takes form of Lindblad equation

[4] Casalderrey-Solana, Teaney: Phys. Rev. D 74 (2006) 085012

Lindblad Equation

$$\frac{\mathrm{d}\rho(t)}{\mathrm{d}t} = -i[H, \rho(t)] + \sum_n \left(C_i^n \rho(t) C_i^{n\dagger} - \frac{1}{2} \left\{ C_i^{n\dagger} C_i^n, \rho(t) \right\} \right)$$

where H is the quarkonium Hamiltonian, and the C^n are collapse operators resulting from interactions with the medium

$$\rho = \begin{pmatrix} \rho_s & 0 \\ 0 & \rho_o \end{pmatrix}, \quad H = \begin{pmatrix} h_s & 0 \\ 0 & h_o \end{pmatrix} + \frac{r^2}{2}\gamma \begin{pmatrix} 1 & 0 \\ 0 & \frac{N_c^2-2}{2(N_c^2-1)} \end{pmatrix},$$

$$C_0^i = \sqrt{\frac{\kappa}{N_c^2-1}} r^i \begin{pmatrix} 0 & 1 \\ \sqrt{N_c^2-1} & 0 \end{pmatrix}, \quad C_1^i = \sqrt{\frac{(N_c^2-4)\kappa}{2(N_c^2-1)}} r^i \begin{pmatrix} 0 & 0 \\ 0 & 1 \end{pmatrix}$$

medium interactions specified by κ and γ

Transport Coefficients

- κ is the heavy quark momentum diffusion coefficient; γ is its dispersive counterpart
- κ and γ related to in-medium width and mass shift of $\Upsilon(1S)$:

$$\Gamma(1S) = 3a_0^2\kappa, \quad \delta M(1S) = \frac{3}{2}a_0^2\gamma,$$

  and accessible from unquenched lattice measurements of Γ and δM
- temperature dependent $\kappa(T)$ can be extracted from chromo-electric correlation functions measurable on the lattice which suffer from severe UV noise
  - currently, multilevel algorithm allows for noise reduction with pure gauge backgrounds, i.e., quenched measurements
  - in the future, gradient flow will allow for noise reduction with full QCD, i.e., unquenched measurements

Extraction of κ

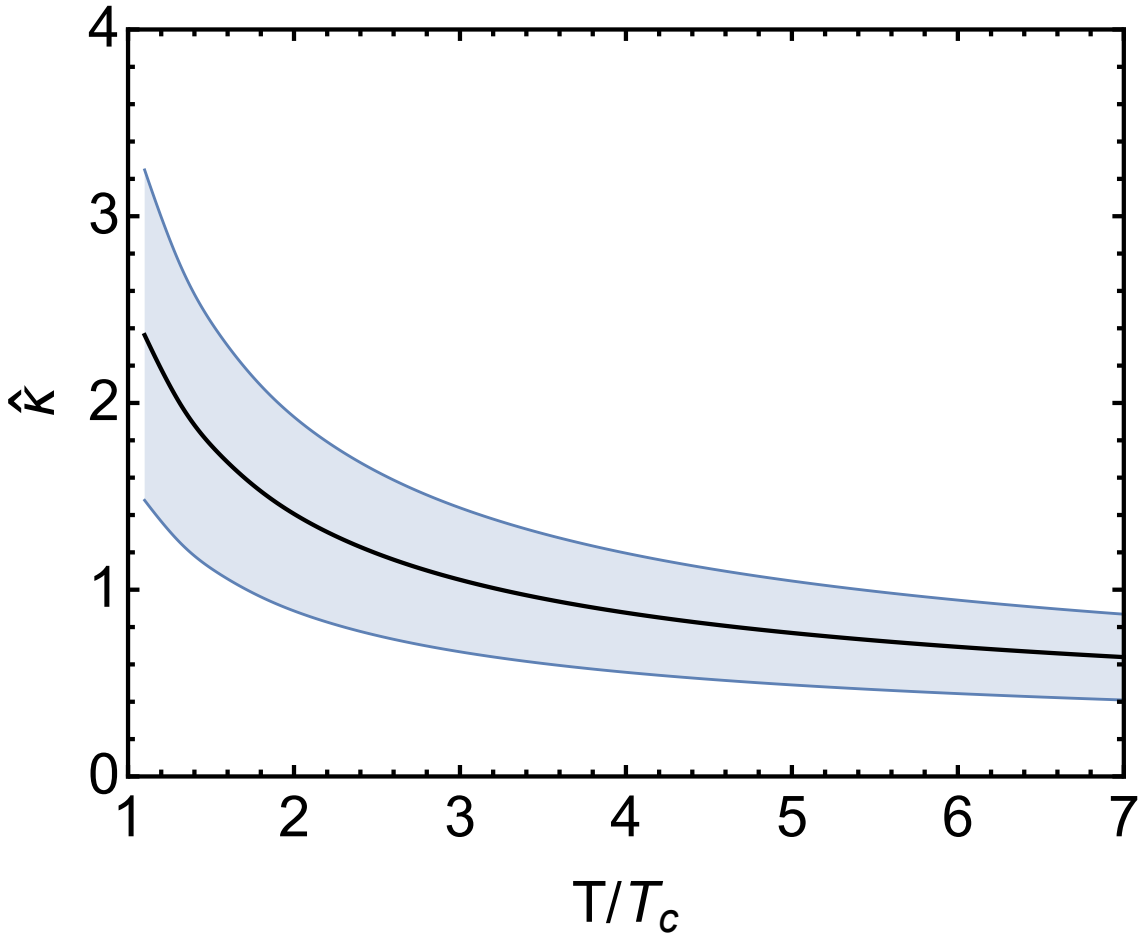

Figure: Direct, quenched lattice measurement of $\hat{\kappa} = \kappa / T^3$ (Brambilla, Leino, Petreczky, Vairo: Phys. Rev. D 102, 074503 (2020)).

We solve the Lindlbad equation using the upper, central, and lower $\hat{\kappa}(T) = \kappa(T)/T^3$ curves.

Extraction of γ

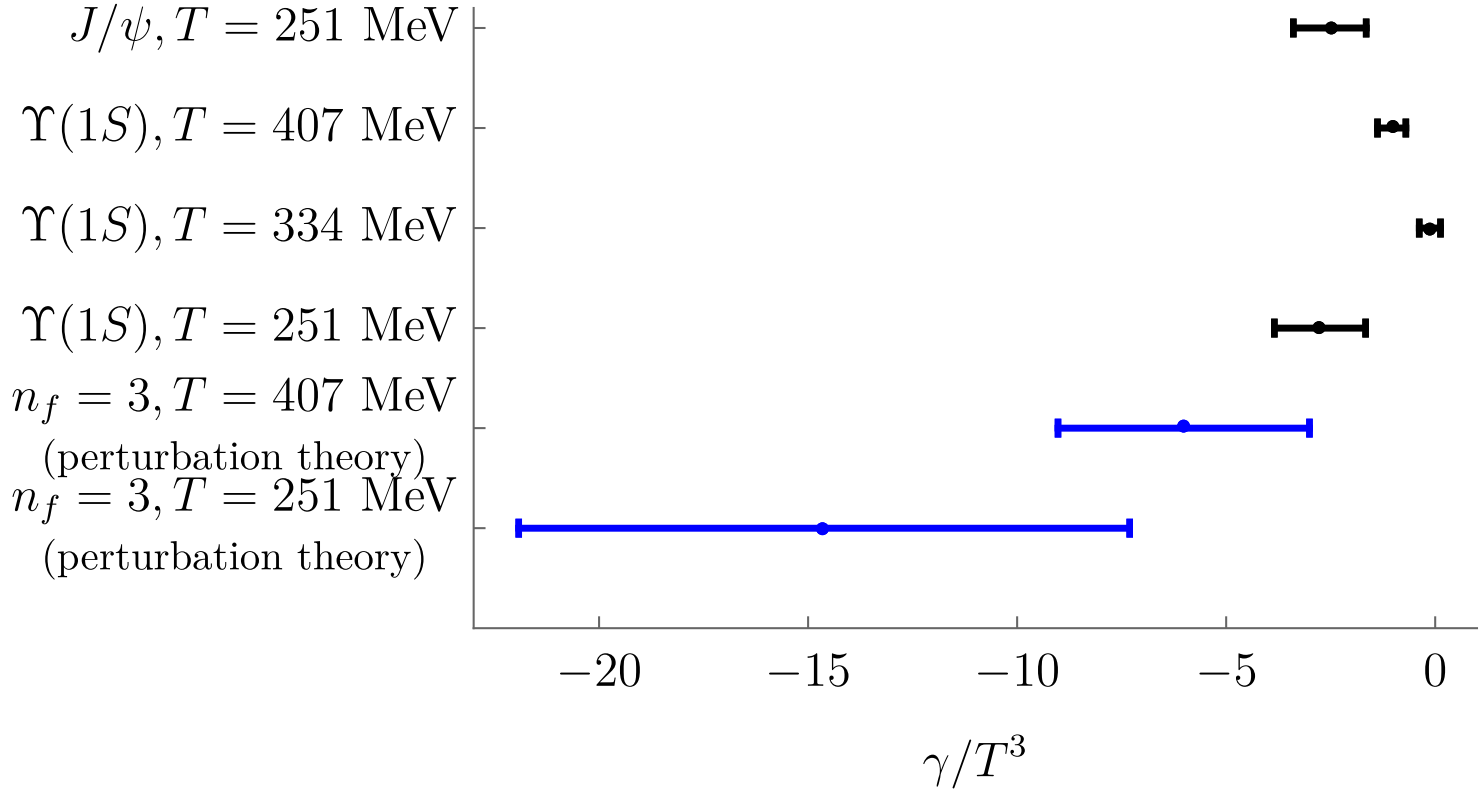

Figure: Indirect extractions of $\hat{\gamma} = \gamma/T^3$ from unquenched lattice measurements of $\delta M(1S)$ (lattice extractions of $\delta M(1S)$ from JHEP 11 (2018) 088 (Kim, Petreczky, Rothkopf) and Phys.Rev.D 100 (2019) 7, 074506 (Larsen, Meinel, Mukherjee, Petreczky).

We solve the Lindlbad equation using
$\hat{\gamma} = \gamma/T^3 = \{-3.5, -1.75, 0\}$.

Quantum Trajectories Algorithm

- Monte Carlo method to solve the Lindblad equation
- less memory intensive due to use of wave function $|\psi\rangle$ rather than density matrix ρ
- absorb quantum number conserving diagonal evolution terms of Lindblad equation into a non-Hermitian effective Hamiltonian

$$H_{eff} = H - \frac{i}{2}\sum_n C_n^\dagger C_n$$

Lindblad equation becomes

$$\frac{\mathrm{d}\rho(t)}{\mathrm{d}t} = -i\left(H_{eff}\,\rho(t) - \rho(t)H_{eff}^\dagger\right) + \sum_n C_i^n \rho(t) C_i^{n\dagger}$$

- H_{eff} term reduces trace of ρ and preserves quantum numbers of state
- C_n term changes quantum numbers of state and ensure overall evolution is trace preserving

H_{eff} Evolution

- evolve wavefunction with H_{eff}

$$|\psi(t+\delta t)\rangle = (1 - iH_{eff}\delta t)|\psi(t)\rangle$$

- H_{eff} evolution preserves quantum numbers of the state and decreases its norm

$$\begin{aligned}\langle\psi(t+\delta t)|\psi(t+\delta t)\rangle &\approx 1 - i\langle\psi(t)|(H_{eff} - H_{eff}^{\dagger})|\psi(t)\rangle\delta t \\ &= 1 - \delta p\end{aligned}$$

  where

$$\delta p = \sum_n \langle\psi(t)|C_n^{\dagger}C_n|\psi(t)\rangle\delta t = \sum_n \delta p_n$$

- decrease in norm related to probability a change of quantum numbers, implemented by $C_n|\psi(t)\rangle$, occurs

Monte Carlo

(normalized) evolution of state

$$|\tilde{\psi}(t+\delta t)\rangle = \begin{cases} \frac{|\psi(t+\delta t)\rangle}{\sqrt{1-\delta p}} & \text{with probability } 1-\delta p \\ \frac{C_n|\psi(t)\rangle}{\sqrt{\delta p_n/\delta t}} & \text{with probability } \delta p \end{cases}$$

i.e., with probability $1-\delta p$, the state evolves as governed by H_{eff}, and with probability δp, is acted on by the collapse operator C_n

simulation

- generate a random number $0 < r_1 < 1$
- evolve state with H_{eff} until norm squared $< r_1$
- generate additional random number(s) to determine which collapse operator C_n to apply

Equivalence of Evolution and Convergence

equivalence of evolution

$$\begin{aligned}\rho(t+\delta t) =& (1-\delta p)\frac{|\psi(t+\delta t)\rangle}{\sqrt{1-\delta p}}\frac{\langle\psi(t+\delta t)|}{\sqrt{1-\delta p}} \\ &+ \delta p \sum_n \frac{\delta p_n}{\delta p}\frac{C_n|\psi(t)\rangle}{\sqrt{\delta p_n/\delta t}}\frac{\langle\psi(t)|C_n^\dagger}{\sqrt{\delta p_n/\delta t}} \\ =& \rho(t) - i[H_{eff}\rho(t) - \rho(t)H_{eff}^\dagger]\delta t + \sum_n C_n\rho(t)C_n^\dagger\delta t,\end{aligned}$$

as given by Lindblad equation

convergence

- calculate expectation values using evolved state
- evolve many states and average to converge to result of directly solving the Lindblad equation

QTraj Implementation[5]

1. initialize wave function $|\psi(t_0)\rangle$
2. generate random number $0 < r_1 < 1$, evolve with H_{eff} until

$$|| \, e^{-i \int_{t_0}^{t} dt' H_{\text{eff}}(t')} |\psi(t_0)\rangle \, ||^2 \leq r_1,$$

   and initiate a quantum jump
3. quantum jump
   - 3.1 if singlet, jump to octet; if octet, generate random number $0 < r_2 < 1$ and jump to singlet if $r_2 < 2/7$; otherwise, remain in octet
   - 3.2 generate random number $0 < r_3 < 1$; if $r_3 < l/(2l+1)$, $l \to l-1$; otherwise, $l \to l+1$.
   - 3.3 multiply wavefunction by r and normalize
4. Continue from step 2.

[5] Ba Omar, et. al.: Comput. Phys. Commun. 273 (2022) 108266

Code Output to Experimental Observables

- each realization of the `QTraj` algorithm is a *quantum trajectory*
- average of N quantum trajectories tends toward the solution of the Lindblad equation as $N \to \infty$
- overlap of resulting average trajectory with eigenstates, e.g., $\Upsilon(1S)$, $\Upsilon(2S)$, etc., used to compute survival probability of that state
- after accounting for feed down of excited states, results can be compared to experiment

Medium Interaction

- medium evolution implemented using a $3+1$D dissipative relativistic hydrodynamics code using a realistic equation of state fit to lattice QCD measurements
- approximately $7-9\times10^5$ physical trajectories
  - production point sampled in transverse plane using nuclear binary collision overlap profile $N_{AA}^{\text{bin}}(x,y,b)$, initial p_T from an E_T^{-4} spectrum, and ϕ uniformly in $[0,2\pi)$
  - 50-100 quantum trajectories per physical trajectory
  - allows for extraction of differential obserables including v_2 and results as a function of transverse momentum p_T
- vacuum evolution from initialization at $t_0=0$ fm until initialization of interaction with medium at $t=0.6$ fm and vacuum evolution for $T<T_f=250$ MeV
  - for $\pi T\gg E$, Lindblad equation accurate at relative order $(rT)^2$ neglecting effects of order $(rT)^2(E/T)$ and higher
  - for $\pi T\lesssim E$, vacuum evolution accurate up to corrections of relative order $(rT)^2$

R_{AA} vs. Centrality

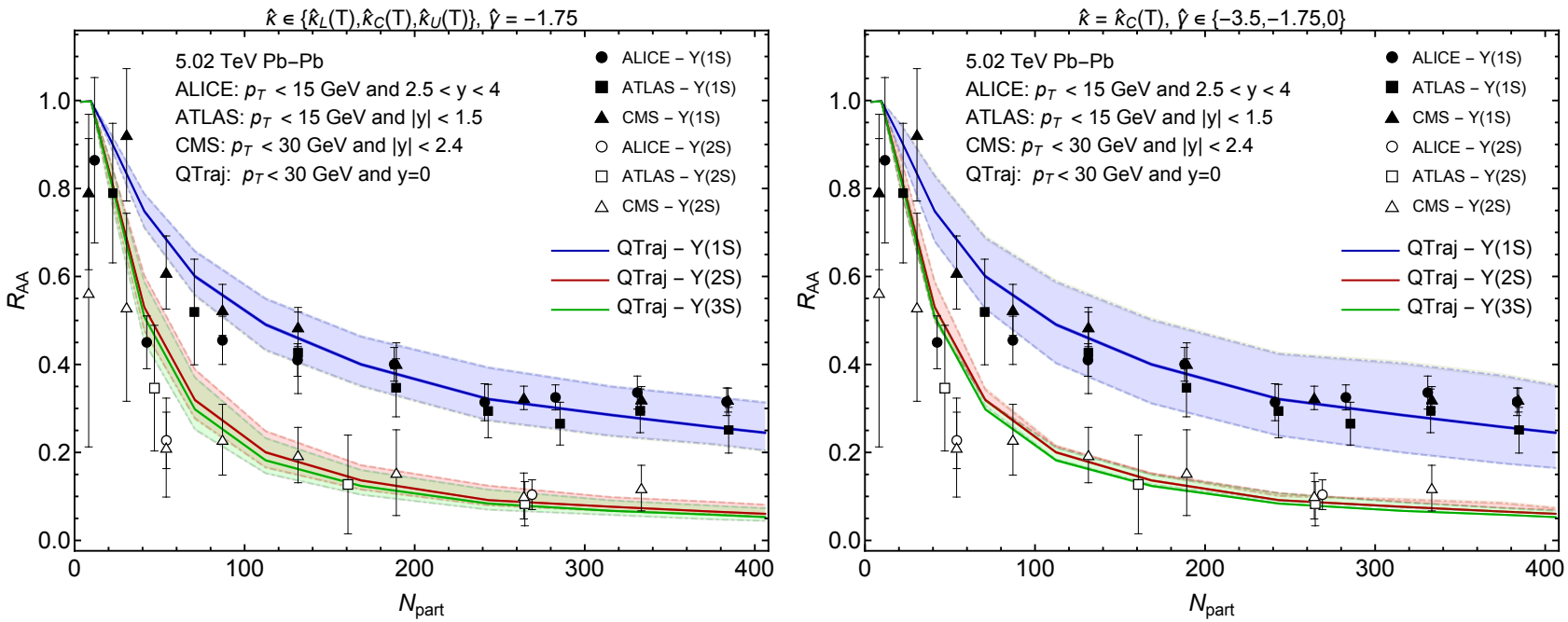

Figure: The nuclear modification factor R_{AA} of the $\Upsilon(1S)$, $\Upsilon(2S)$, $\Upsilon(3S)$ as a function of centrality compared to experimental measurements. The bands in the left plot represent variation of $\hat{\kappa}$ at fixed $\hat{\gamma} = -1.75$; the bands in the right plot represent variation of $\hat{\gamma}$ at fixed $\hat{\kappa} = \hat{\kappa}_C$.

Double Ratio $2S$ vs. Centrality

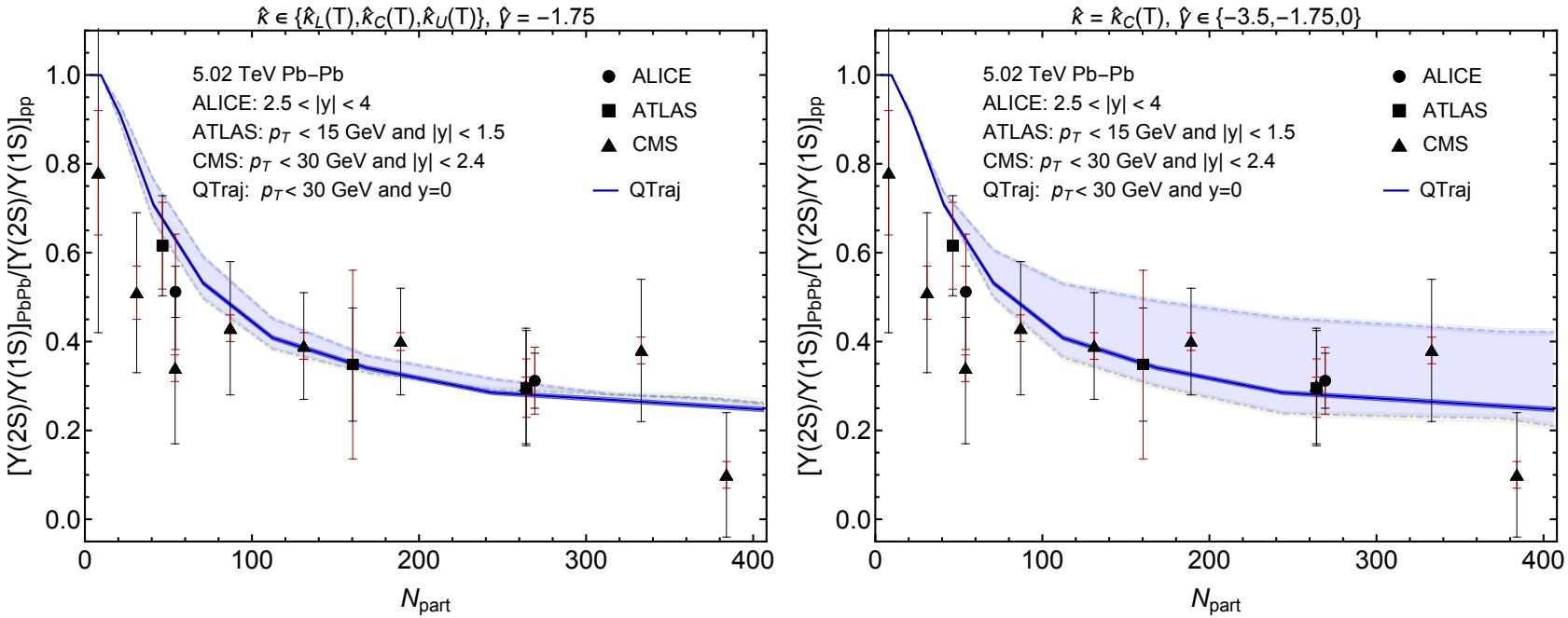

Figure: Ratio of $R_{AA}(2S)$ to $R_{AA}(1S)$ computed in QTraj compared to experimental results. The bands in the left plot represent variation of $\hat{\kappa}$ at fixed $\hat{\gamma} = -1.75$; the bands in the right plot represent variation of $\hat{\gamma}$ at fixed $\hat{\kappa} = \hat{\kappa}_C$. The black and red bars in the experimental data represent statistical and systematic uncertainties, respectively.

Double Ratio 3S vs. Centrality

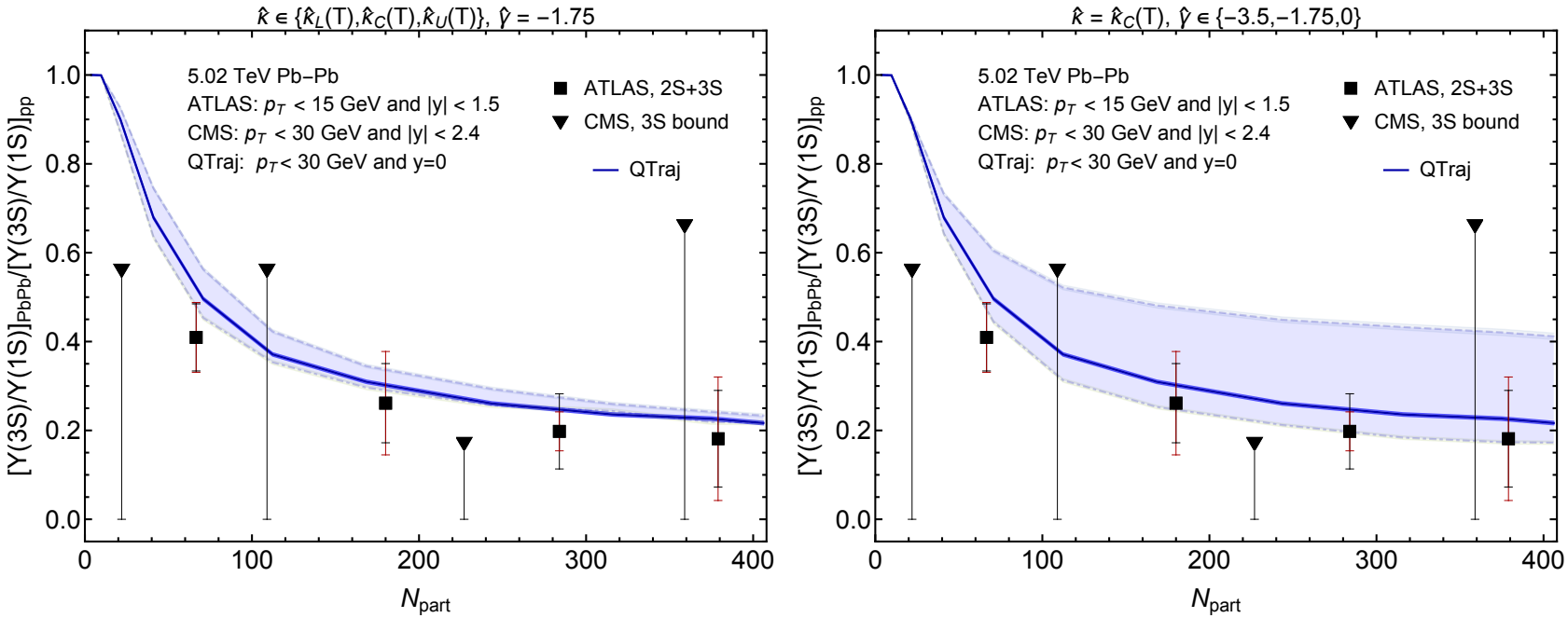

Figure: Ratio of $R_{AA}(2S)$ to $R_{AA}(1S)$ computed in QTraj compared to experimental results. The bands in the left plot represent variation of $\hat{\kappa}$ at fixed $\hat{\gamma} = -1.75$; the bands in the right plot represent variation of $\hat{\gamma}$ at fixed $\hat{\kappa} = \hat{\kappa}_C$. The black and red bars in the experimental data represent statistical and systematic uncertainties, respectively.

R_{AA} vs. p_T

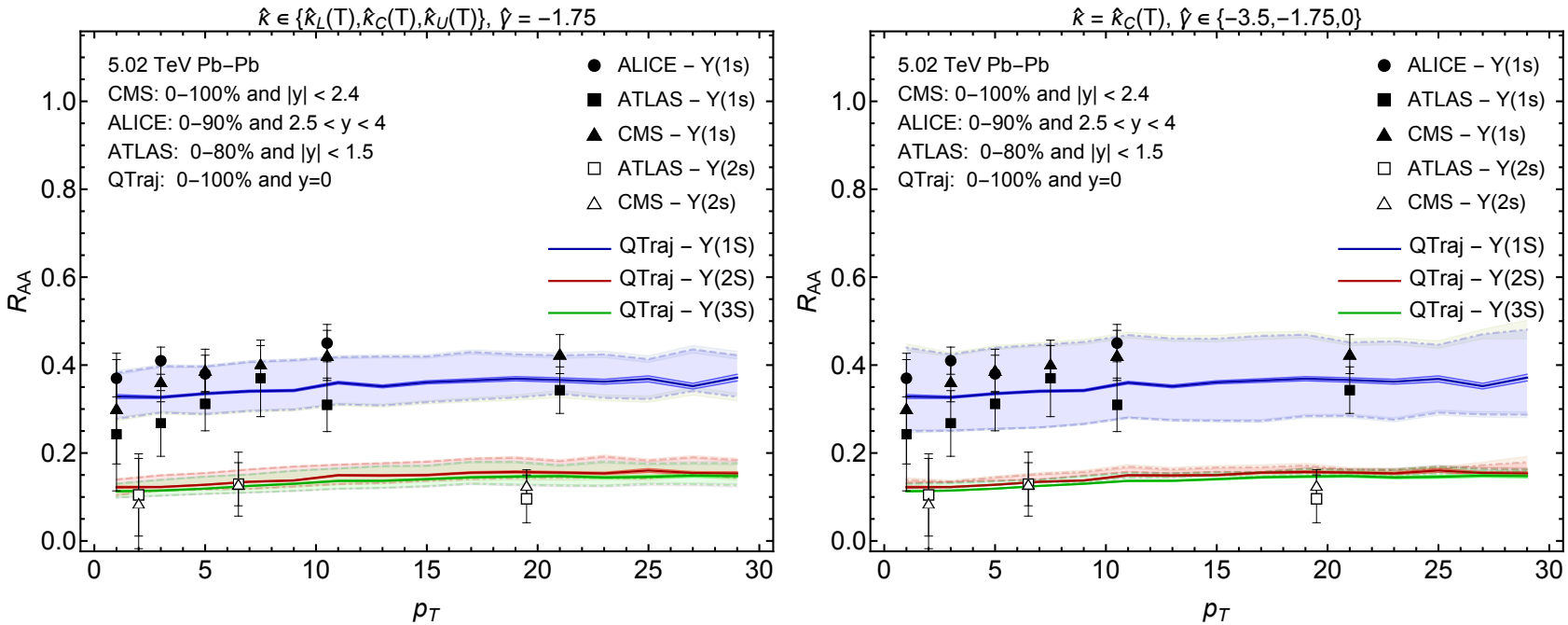

Figure: The nuclear modification factor R_{AA} of the $\Upsilon(1S)$, $\Upsilon(2S)$, $\Upsilon(3S)$ as a function of p_T compared to experimental measurements. The bands in the left plot represent variation of $\hat{\kappa}$ at fixed $\hat{\gamma} = -1.75$; the bands in the right plot represent variation of $\hat{\gamma}$ at fixed $\hat{\kappa} = \hat{\kappa}_C$.

Double Ratio $2S$ vs. p_T

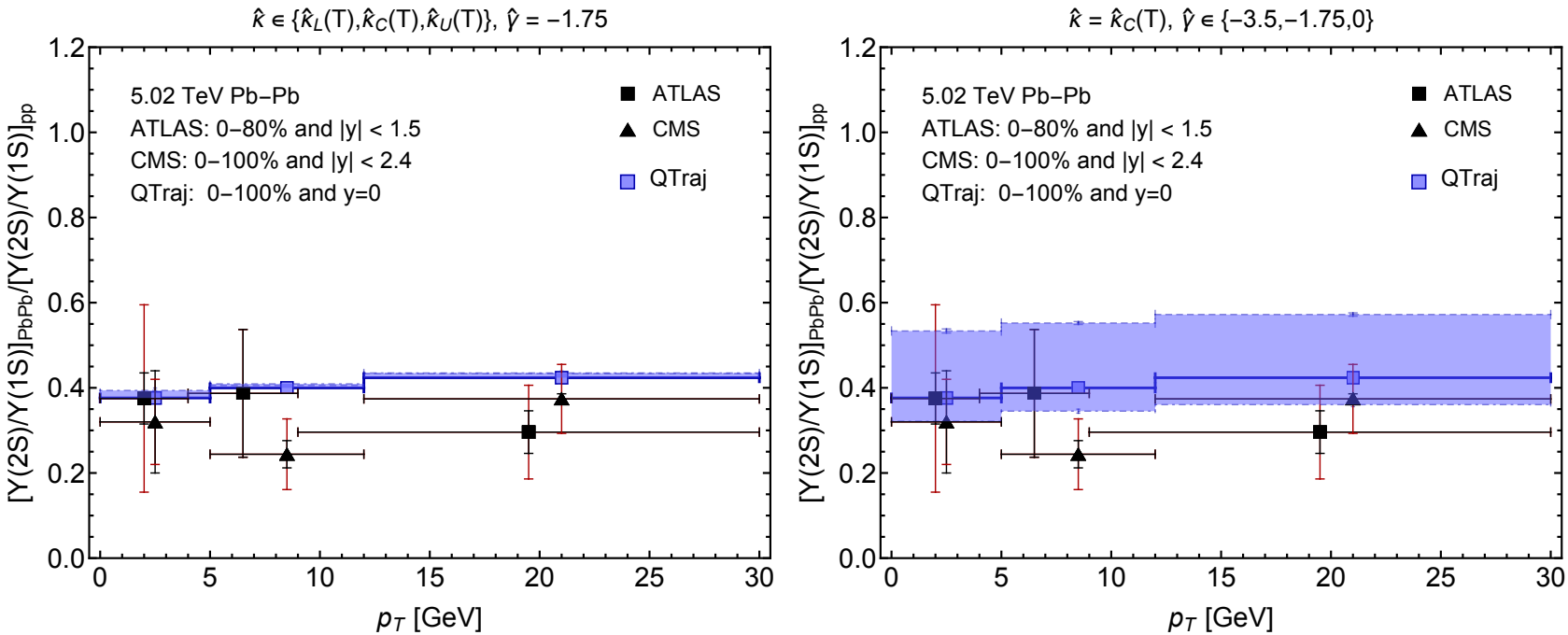

Figure: The double ratio of the nuclear modification factor $R_{AA}[\Upsilon(2S)]$ to $R_{AA}[\Upsilon(1S)]$ as a function of p_T compared to experimental measurements. The bands in the left plot represent variation of $\hat{\kappa}$ at fixed $\hat{\gamma} = -1.75$; the bands in the right plot represent variation of $\hat{\gamma}$ at fixed $\hat{\kappa} = \hat{\kappa}_C$. The black and red bars in the experimental data represent statistical and systematic uncertainties, respectively.

$v_2[\Upsilon(1S)]$ vs. Centrality

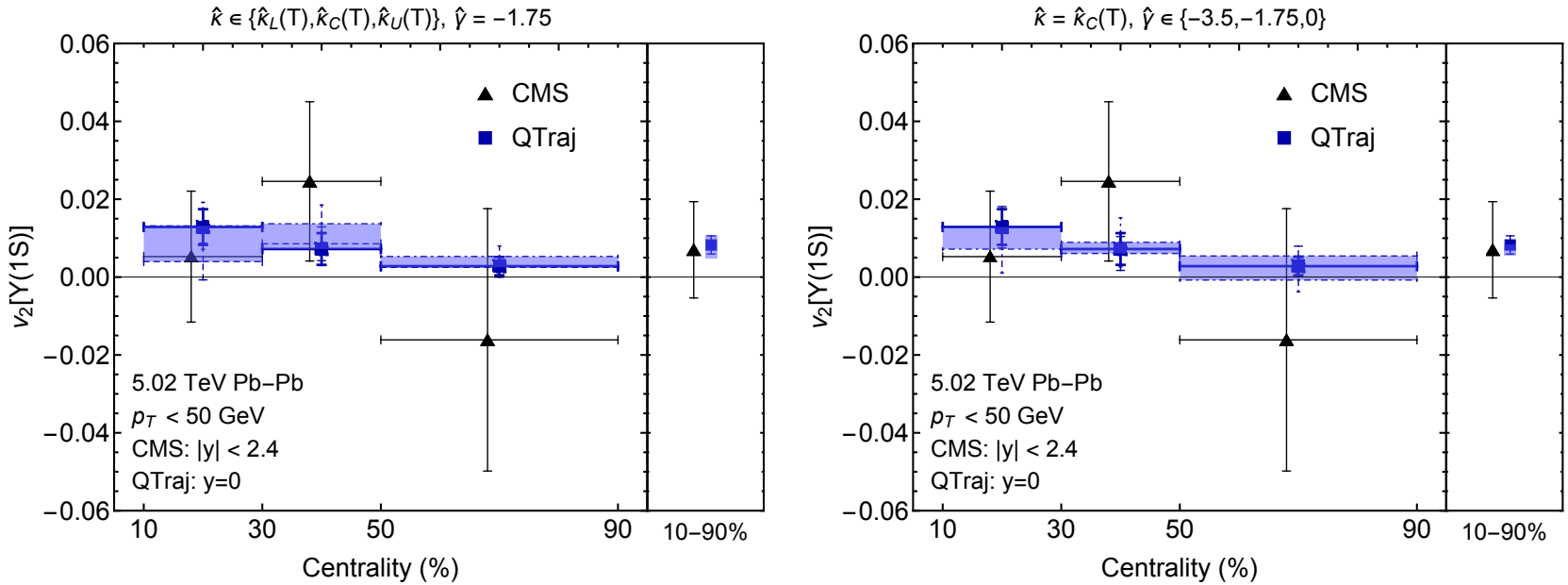

Figure: The elliptic flow v_2 of the $\Upsilon(1S)$ as a function of centrality compared to experimental measurements. The bands in the left plot represent variation of $\hat{\kappa}$ at fixed $\hat{\gamma} = -1.75$; the bands in the right plot represent variation of $\hat{\gamma}$ at fixed $\hat{\kappa} = \hat{\kappa}_C$.

$v_2[\Upsilon(2,3S)]$ vs. Centrality

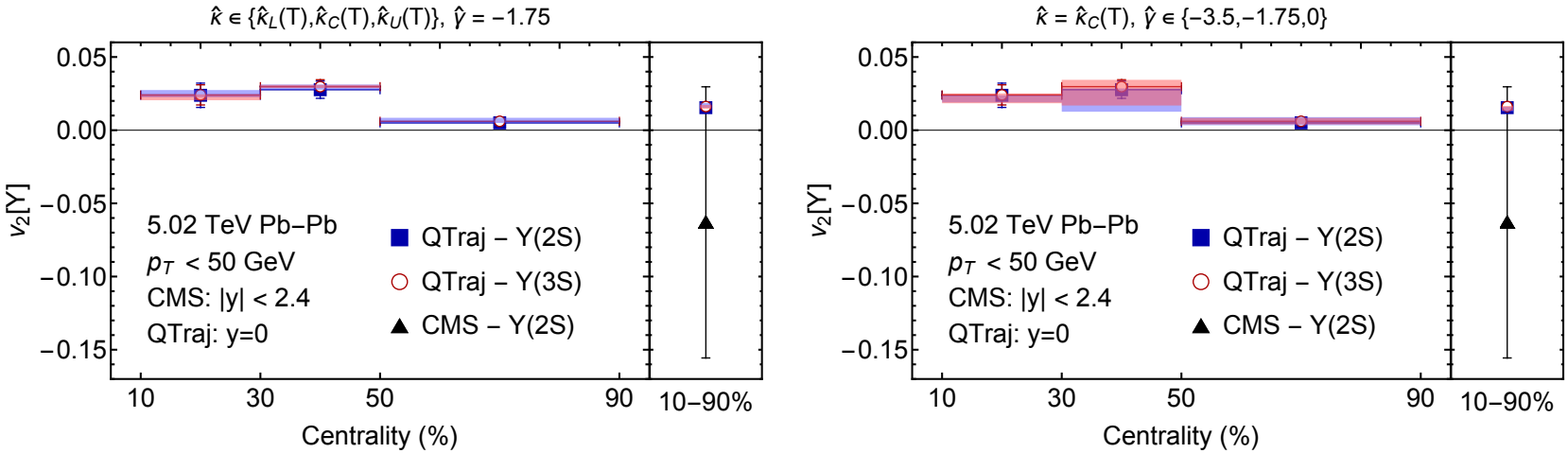

Figure: The elliptic flow v_2 of the $\Upsilon(2S)$ and $\Upsilon(3S)$ as a function of centrality compared to experimental measurements. The bands in the left plot represent variation of $\hat{\kappa}$ at fixed $\hat{\gamma} = -1.75$; the bands in the right plot represent variation of $\hat{\gamma}$ at fixed $\hat{\kappa} = \hat{\kappa}_C$.

$v_2[\Upsilon(1S)]$ vs. p_T

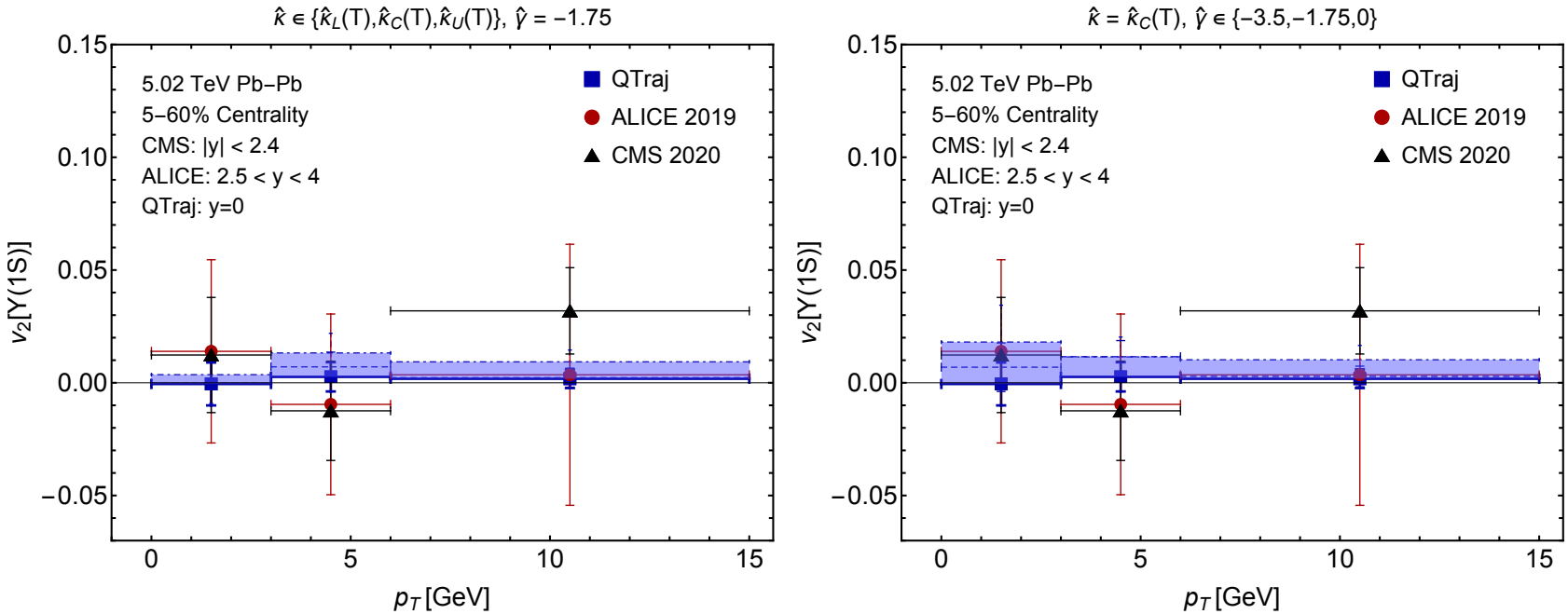

Figure: The elliptic flow v_2 of the $\Upsilon(1S)$ as a function of p_T compared to experimental measurements. The bands in the left plot represent variation of $\hat{\kappa}$ at fixed $\hat{\gamma} = -1.75$; the bands in the right plot represent variation of $\hat{\gamma}$ at fixed $\hat{\kappa} = \hat{\kappa}_C$. The black and red bars in the experimental data represent statistical and systematic uncertainties, respectively.

Experimental References

- Phys. Lett. B 822, 136579 (2021) (ALICE)
- link to presentation (ATLAS)
- Phys. Lett. B 790, 270 (2019) (CMS)
- Phys. Rev. Lett. 120, 142301 (2018) (CMS)
- Phys. Lett. B 819, 136385 (2021) (CMS)
- Phys. Rev. Lett. 123, 192301 (2019) (ALICE)

Summary I

- due to hierarchies of scale, system of in-medium bottomonium ideally suited for description using EFT methods, specifically pNRQCD, and the OQS formalism
- for $M \gg 1/a_0 \gg (\pi)T \gg E$, at first nontrivial order in the multipole expansion and linear order in the heavy quark density, the system realizes quantum Brownian motion, and the evolution equations take the form of a Lindblad equation
- computational methods necessary to solve the Lindblad equation and extract observables including R_{AA} and v_2
- `QTraj` code implements the quantum trajectories algorithm to solve the Lindblad equation and extract R_{AA} and v_2 as functions of N_{part} and p_T
  - results show good agreement with experimental data

Summary II

method and results are

- are fully quantum, non abelian, and heavy quark number conserving
- take into account dissociation and recombination
- depend only on the transport coefficients κ and γ the values of which we take from lattice data

Thank you!